

A New Tool for Large-Area Analysis of Transient Pore Water Pressures in Layered Shallow Covers Prone to Failure

Diana SALCIARINI ^a, Giuseppe C. CASTORINO ^b, Sabatino CUOMO ^b and Claudio TAMAGNINI ^a

^aDepartment of Civil and Environmental Engineering, University of Perugia, Italy

^bLab. of Geotechnics, Department of Civil Engineering, University of Salerno, Italy.

Abstract. In this paper we present a modified version of an existing, physically-based model for shallow landslide susceptibility analysis over large area. In general, the potentially unstable soil cover is considered uniform and homogeneous, over impervious underlying bedrock. In several case studies, this was proven to be unrealistic. The possibility of taking into account the detailed configuration of the soil cover allows having a more accurate estimate of the potentially unstable volumes, which determine the intensity of the considered phenomena. The newly-implemented tool was tested by comparing its results with those obtained from a Finite Element (FE) commercial code, solving the same 1D problem. Then, a parametric analysis was carried out by varying the permeability ratio between the two layers, with the aim of examining the influence of such parameter on the pore-pressure distribution along the vertical profile. As expected, as the permeability ratio increases, the underlying layer tends to behave as an impervious boundary. This increases the chance that only the most superficial soil layer fails. An analysis of the routine performance and efficiency was also done to investigate the response of the model with various tolerances and different spatial discretizations along the vertical profile. As main result, it is shown that the variability in ground conditions may highly affect the pore water pressures and the proposed seepage model can be successfully whether detailed stratigraphy site investigations are available.

Keywords. rainfall-induced landslides, stratigraphic setting, shallow covers, numerical solution

1. Background

In the last decades, due to the availability of new computational tools for landslides susceptibility modeling (Baum et al., 2008; Godt et al., 2008; Baum et al., 2010; Salciarini et al., 2012), scientists and practitioners have begun to be ever more involved in the analysis of slope stability conditions over large area (Cascini et al., 2008, 2011; Cuomo & Della Sala, 2013).

These tools, implemented in GIS platforms, allow taking into account the major hydraulic and mechanical issues related to slope failure, even for unsaturated soils, as well as the spatial variability of both topography and soil properties.

The above-mentioned tools are generally physically-based, are able to perform spatial analyses over a grid-based discretization of a study area starting from a Digital Terrain Model (DTM), and are capable of considering the process evolution within the thickness of the shallow deposit.

A first code capable to account for saturated

soil conditions, steady-state seepage and spatially homogeneous soil was the SHALSTAB model (Montgomery & Dietrich, 1994).

New improvements were later reached in the TRIGRS model (Baum et al., 2008) by including unsaturated conditions and transient seepage, based on a closed form solution of the Richards equation, with the soil characteristic curves defined by Gardner (1958). Here, the equation governing the infiltration process is solved for an infinitely deep impermeable basal boundary, considering at the ground surface a condition of constant flux for a specified time, and zero flux thereafter (Iverson, 2000).

According to the basic assumption made by Iverson (2000), the stratigraphic setting is homogeneous, and the soil thickness is comparable to the square root of the upslope contributing area. Whereas the latter hypothesis is realistic, the former condition is not always fulfilled because the shallow deposits can be formed by air-fall deposits (e.g. pyroclastic volcanic soils or loess) or by weathering of

underlying bedrock.

Although the spatially homogeneous soil limit can be accounted by subdividing a given study area in smaller zones (Sorbino et al. 2007, 2010), rigorous and effective tools to take into account a non-homogeneous stratigraphy are still unavailable. This last feature is a “must have” where the discontinuities in conductivity and shear strength between the layers can be detected and quantified. More recent enhancements were proposed as well. The solution proposed by Iverson (2000) was generalized by Savage et al. (2003) for the case of a time-varying sequence of surface fluxes of variable intensities and durations and a layer of finite thickness.

This paper contributes to the existing research on this topic, by introducing a new tool, written in MATLAB code, which can perform a seepage analysis for shallow covers including the case they are stratified and the layers are characterized by different permeability values. First, three benchmark cases with fine and coarse soils are analyzed for validation, and then perspectives for the use of the new tools are drawn in the framework of landslide risk analysis.

2. The Proposed Model

2.1. The New Tool for Seepage Analysis

In this work the closed-form solution by Srivastava & Yeh (1991) implemented into the original TRIGRS model was substituted with the numerical solution of the partial differential equation of the infiltration process, generalized to a three-phase, deformable porous media:

$$n \frac{\partial S_w}{\partial t} - S_w \frac{\partial \varepsilon_v}{\partial t} + \frac{\partial}{\partial Z} \left[k_s k_r \left(-\frac{\partial \psi}{\partial Z} + \frac{\partial \zeta}{\partial Z} \right) \right] = 0 \quad (1)$$

where S_w is the degree of saturation of the soil, ε_v is the volumetric strain of the solid skeleton, t is the time, Z is the vertical depth, n is the soil porosity ψ is the pressure head, z is the geometric height, k_s is the hydraulic conductivity in saturated conditions, and k_r is the relative hydraulic conductivity.

Eq. (1) governs the infiltration process and controls the pressure head evolution in space and time. The first term of Eq. (1) is related to the

time variation of the degree of saturation:

$$\begin{aligned} n \frac{\partial S_w}{\partial t} &= n \frac{\partial S_w}{\partial \psi} \frac{\partial \psi}{\partial t} = n \frac{\partial S_w}{\partial \psi} \gamma_w \frac{\partial (u_w / \gamma_w)}{\partial t} = \\ &= n \frac{\partial S_w}{\partial \psi} \frac{\partial u_w}{\partial t} = \tilde{C}_s \frac{\partial u_w}{\partial t} \end{aligned} \quad (2)$$

where $\tilde{C}_s = n \partial S_w / \partial u_w$, and it is null if the soil is in saturated condition.

The solid skeleton constitutive equation follows and controls both the deformability and the material strength.

$$\varepsilon_v \cong \varepsilon_z = \frac{1}{E_{ed}} \sigma''_z \quad (3a)$$

$$\sigma''_z = \sigma_z - S_w \gamma_w \psi \quad (3b)$$

where the E_{ed} is the oedometric module of the soil, while σ''_z is the effective stress defined by Bishop. The second term of Eq. (1) accounts for the volumetric deformation of the solid skeleton:

$$\begin{aligned} S_w \frac{\partial \varepsilon_v}{\partial t} &= \frac{S_w}{E_{ed}} \frac{\partial \sigma''_z}{\partial t} = \frac{S_w}{E_{ed}} \frac{\partial}{\partial t} (\sigma_z - S_w \gamma_w \psi) = \\ &= -\frac{S_w}{E_{ed}} \left(\psi \frac{\partial S_w}{\partial \psi} + S_w \right) \gamma_w \frac{\partial \psi}{\partial t} = \\ &= -\frac{S_w}{E_{ed}} \left(u_w \frac{\partial \psi}{\partial u_w} + S_w \right) \frac{\partial u_w}{\partial t} \end{aligned} \quad (4)$$

and it is null under the assumption of rigid solid skeleton. Finally, the last term of Eq. (1) can be written as follows:

$$\begin{aligned} \frac{\partial}{\partial Z} \left[k_s k_r \left(-\frac{\partial \psi}{\partial Z} + \frac{\partial \zeta}{\partial Z} \right) \right] &= \frac{\partial}{\partial Z} \left[k_s k_r \left(-\frac{1}{\gamma_w} \frac{\partial u_w}{\partial Z} + \right. \right. \\ &\left. \left. + \frac{\partial \zeta}{\partial Z} \right) \right] = \frac{\partial}{\partial Z} \left[k_s k_r \left(\frac{1}{\gamma_w} \frac{\partial u_w}{\partial Z} + G \right) \right] \end{aligned} \quad (5)$$

where G is equal to $\delta \zeta / \delta Z$ and it is set to -1 for horizontal ground surface.

Replacing the Eqs. (3), (4) and (5) into Eq. (1) it is possible to re-formulate the governing equation into the following parabolic partial differential equation (Salciarini & Tamagnini, 2014):

$$\left[\mathcal{L}_s^0 + \frac{S_w}{E_{ed}} \left(u_w \frac{\partial \mathcal{L}_s^0}{\partial n} + S_w \right) \right] \frac{\partial u_w}{\partial t} - \frac{\partial}{\partial Z} \left[\frac{k_s k_r}{\gamma_w} \left(\frac{\partial u_w}{\partial Z} + G \right) \right] = 0 \quad (6)$$

in which the term on the right hand represents the flux amount, and the other terms are shown in the following, by introducing the Gardner’s (1958) hydraulic conductivity function:

$$\mathcal{L}_s^0 = n \frac{\partial S_w}{\partial u_w} = \frac{n\beta}{\gamma_w} (1 - S_{wr}) \exp \left(\beta \frac{u_w}{\gamma_w} \right) \quad (7)$$

$$S_w = S_{wr} + (1 - S_{wr}) \exp \left(\beta \frac{u_w}{\gamma_w} \right) \quad (8)$$

$$k_r = \exp \left(\beta \frac{u_w}{\gamma_w} \right) \quad (9)$$

In the case of a layered cover, all the above-mentioned parameters change with properly depth functions.

To solve Eq. (6) a MATLAB-integrated function, called PDE-PE (Partial Differential Equation – Parabolic Equation), is used. It solves initial-boundary value problems for systems of parabolic and elliptic PDEs in the one-space variable x and time t .

$$c \left(x, t, u, \frac{\partial u}{\partial x} \right) = x^{-m} \frac{\partial}{\partial x} \left[x^m f \left(x, t, u, \frac{\partial u}{\partial x} \right) \right] + s \left(x, t, u, \frac{\partial u}{\partial x} \right) \quad (10)$$

where $t_0 \leq t \leq t_f$ and $a \leq x \leq b$. The interval $[a, b]$ must be finite and m can be 0, 1, or 2, respectively for slab, cylindrical, or spherical symmetry.

In Eq. (10), $f(x, t, u, \partial u/\partial x)$ is a flux term and $s(x, t, u, \partial u/\partial x)$ is a source term. The coupling of the partial derivatives with respect to time is restricted to multiplication by a diagonal matrix $c(x, t, u, \partial u/\partial x)$. The diagonal elements of this matrix are either identically zero for an elliptic problem, otherwise they are positive for a parabolic equation.

In general, Ordinary Differential Equations (ODEs) resulting from space discretization can

be integrated to obtain approximate solutions at specified times. The solution components have to satisfy initial conditions (for $t = t_0$ and all x) in the following form:

$$u(x, t_0) = u_0(x) \quad (11)$$

Furthermore, the solution components have to satisfy the boundary conditions in $x = a$ or $x = b$ in the form:

$$p(x, t, u) + q(x, t) f \left(x, t, u, \frac{\partial u}{\partial x} \right) = 0 \quad (12)$$

Consequently, Eq. (6) can be considered as a parabolic partial differential equation with slab symmetry, without source term ($s=0$) and flux and c terms respectively at the right and left part of the equation, in which the u and x terms of Eq. (11) are respectively equal to u_w and Z .

2.2. Slope Stability Module

On hillslopes covered by colluvial or volcanic soil with limited thickness compared to the length of the slope, the infinite slope stability hypothesis can be assumed. The ratio between the available shear strength τ_f of the soil along the potential failure plane, given by the Mohr–Coulomb failure criterion, and the driving stress τ_d , is called factor of safety FS :

$$FS = \frac{\tan \phi' + \frac{c' - \psi(Z, t) \gamma_w \tan \phi'}{\gamma_s d_{lb} \sin \alpha \cos \alpha}}{\tan \alpha} \quad (13)$$

where ϕ' is the soil friction angle for effective stress, c' is the effective cohesion, ψ is the pressure head, Z is the vertical coordinate, t is the time, d_{lb} is the depth of the lower boundary, α is the slope steepness, and γ_w and γ_s are respectively the unit weights of water and soil.

For a stratified shallow cover, Eq. (13) for the lower layer is given by:

$$FS = \frac{c'_2 + \cos^2 \alpha \left[\gamma_{s,1} h_1 + \gamma_{s,2} (Z - h_1) \right] \tan \phi'_2 + \cos^2 \alpha \left[\psi(Z, t) \gamma_w \right] \tan \phi'_2}{\left[\gamma_{s,1} h_1 + \gamma_{s,2} (Z - h_1) \right] \sin \alpha \cos \alpha} \frac{1}{\left[\gamma_{s,1} h_1 + \gamma_{s,2} (Z - h_1) \right] \sin \alpha \cos \alpha} \quad (14)$$

An infinite slope is considered stable when $FS > 1$, and in the limiting equilibrium condition when $FS = 1$. The depth Z where FS reaches the value 1 is the depth of landslide triggering at time t .

3. Model Validation

The proposed model was validated performing a comparison with the results provided by the commercial code SEEP/W, (GeoSlope, 2005), for the same 1D-problem.

An ideal column of soil (see Fig. 1) with a depth $h = 3.0$ m, was analysed, considering three different cases:

1. homogeneous coarse-grained material, with hydraulic conductivity in saturated condition equal to $k_s = 5.0e^{-5}$ m/s (Fig. 1a);
2. homogeneous fine-grained material, with hydraulic conductivity in saturated condition equal to $k_s = 1.0e^{-7}$ m/s (Fig. 1b);
3. layered cover with a coarse-grained material at the top ($k_s = 5.0e^{-5}$ m/s) for a depth $h_1 = 1.0$ m and a fine-grained material at the bottom ($k_s = 3.0e^{-6}$ m/s) for a depth $h_2 = 2.0$ m (Fig. 1c).

All the simulations were performed considering a rainfall duration of 12 hours and a rainfall rate of $2.78e^{-6}$ m/s. The initial position of the water table was, for all the three cases, at the column base. In Tab. 1 the adopted values for the three study cases are shown.

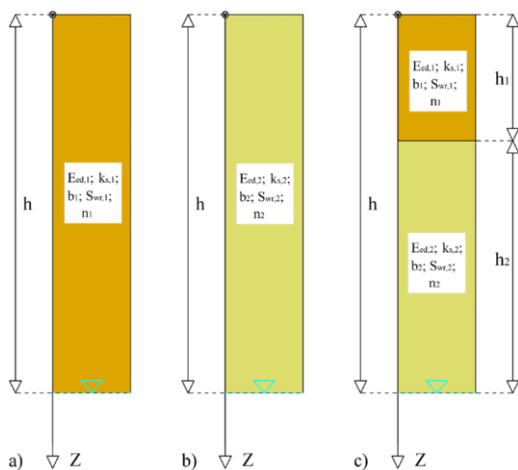


Figure 1. Sketches of the three cases analyzed in 1D-conditions: a) coarse-grained cover, b) fine-grained cover, c) layered cover.

Table 1. Material properties.

Material	k_s (m/s)	n (-)	θ_r (-)	c' (kPa)	ϕ' (°)	γ_s kN/m ³
Coarse	$5e^{-5}$	0.68	0.15	0	38	14.5
Fine	$3e^{-6}$	0.51	0.1	5	35	18.0

$q = 10\text{mm/h}$, $t_d = 12\text{h}$, $b = 1\text{m}^1$, $\alpha = 30^\circ$

3.1. Results

The results of all the simulations are shown in Figs. 2, 3 and 4, in terms of: pressure head, degree of saturation and safety factor evolution with time. Each graph includes the comparison between the model predictions (solid lines) and the SEEP/w predictions (circular markers).

Figs. 2 and 3 shows the results for the case of homogeneous column of coarse-grained and fine-grained soils, respectively. It can be noticed that the solutions provided by the proposed model, in solid lines, are approximately overlaid to that obtained from the SEEP/W model, in circular markers.

Fig. 4 shows the results for the case of layered cover, evidencing how the proposed model is stable also at the contact between layers, where the FEM model does not reach the convergence to compute the degree of saturation ($S_{w,s}$). For all the comparisons shown, the differences in terms of pressure head, degree of saturation and safety factor evolution, in space and time are relatively negligible.

The numerical efficiency of the model on the computation of the pressure head (ψ) was evaluated varying the computational tolerance (TOL) and the space discretization along the vertical ΔZ .

As shown in Tab. 2, passing from a TOL of $1.0e^{-12}$ to a TOL of $1.0e^{-5}$, the safety factor is significantly not influenced. Whereas, decreasing the TOL until $1.0e^{-1}$ the safety factor value can vary up to the 7% from the value obtained with a TOL of $1.0e^{-5}$.

Also, for the analyzed cases, the safety factor is not very susceptible to a decrease of ΔZ along the vertical, which should conduct to a more rigorous solution but, from the computational point of view, it is more time consuming.

Table 2. Performance of the proposed model, evaluated with reference to the minimum computed Factor of Safety (FS).

FS _{min}	Tolerance on pressure head computation (m)									
	1e ⁻¹²	1e ⁻⁵	1e ⁻¹	1e ⁻¹²	1e ⁻⁵	1e ⁻¹	1e ⁻¹²	1e ⁻⁵	1e ⁻¹	
Δz (m)	Coarse			Fine			Coarse-Fine			
	0.05	1.255	1.255	1.344	1.345	1.345	1.324	1.330	1.330	1.347
	0.10	1.256	1.256	1.210	1.345	1.345	1.343	1.331	1.331	1.347
0.20	1.256	1.256	1.250	1.345	1.345	1.343	1.332	1.332	1.331	

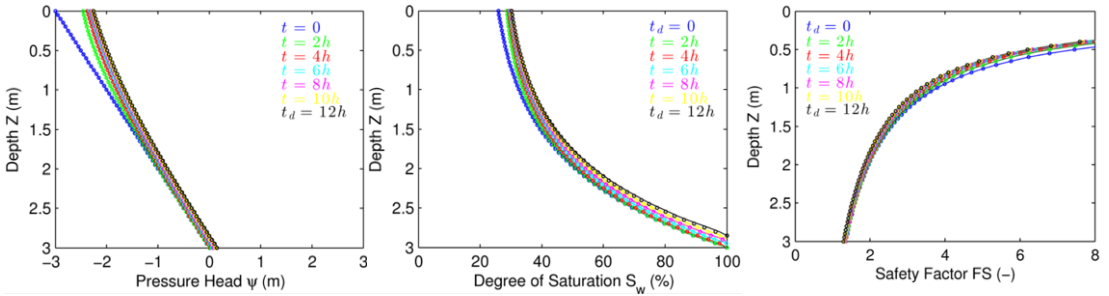


Figure 2. Variation of pressure head (p, m), saturation degree (S_w, %) and factor of safety (FS) with depth Z (m) for uniform column of coarse material in figure 1a. Results of the proposed model in solid lines, FEM results indicated with dots.

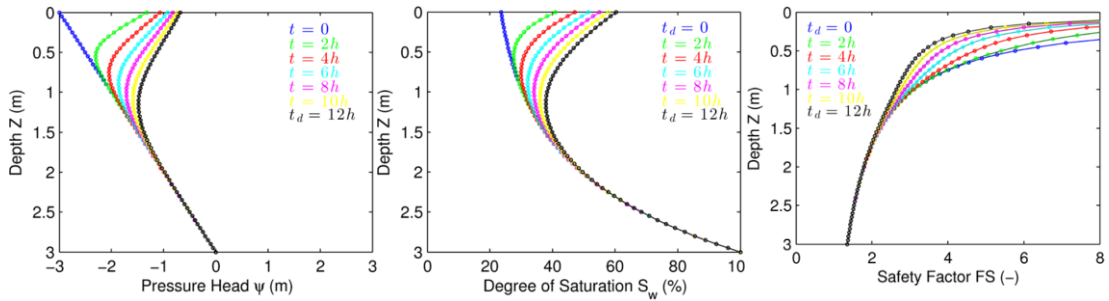


Figure 3. Variation of pressure head (p, m), saturation degree (S_w, %) and factor of safety (FS) with depth Z (m) for uniform column of fine material in figure 1b. Results of the proposed model in solid lines, FEM results indicated with dots.

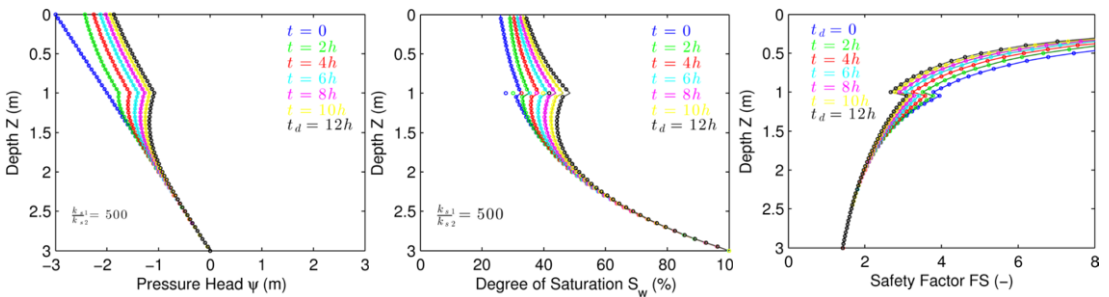


Figure 4. Variation of pressure head (p, m), saturation degree (S_w, %) and factor of safety (FS) with depth Z (m) for the stratified column of figure 1c. Results of the proposed model in solid lines, FEM results indicated with dots.

Fig. 5 represents on the x and y-axis, respectively, the pore water pressure values computed by the SEEP/w code and those obtained from the proposed model.

The points on the diagonal represent a perfect agreement between the computed pore

water pressures by the two models, for the three considered cases. This graph highlights that the differences are always negligible both in the case of homogeneous (coarse-grained or fine-grained) cover, and in the case of layered cover.

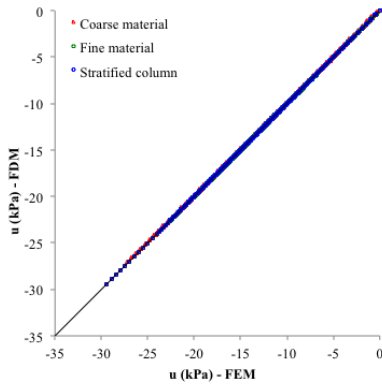


Figure 5. Comparison of the results computed by the proposed model and the SEEP/w code.

4. Conclusion

In this paper a new physically-based model for simulating the pore pressure evolution – and consequently, the safety factor evolution – in homogeneous and layered covers is presented. The model numerically solves the partial differential equation of the infiltration process, generalized to a three-phase, deformable porous media (Richards, 1931). The model was validated by comparing its results with those obtained from the SEEP/w commercial code. Such validation showed a practically null divergence between the results provided by the two tools. Also a parametric study on the computational efficiency of the model performance was presented, showing a low affection of the spatial discretization on the results. Starting from such encouraging results, the possible perspective of the model is to extend the analysis from the 1D-problems to the analysis of the transient water pressures evolution over large areas.

Acknowledgements

The financial support of the Project PRIN 2010-2011 “La mitigazione del rischio da frana mediante interventi sostenibili” funded by the *Italian Ministry of University and Research* is gratefully acknowledged.

References

Baum, R.L., Godt, J.W., Savage, W. Z. (2010). Estimating the timing and location of shallow rainfall-induced landslides using a model for transient, unsaturated

infiltration, *Journal of Geophysical Research: Earth Surface* (2003–2012), **115** (F3).

- Baum, R.L., Savage, W.Z., Godt, J.W. (2008). TRIGRS - a Fortran program for transient rainfall infiltration and grid-based regional slope-stability analysis, version 2.0, *USGS Open File Report 08–1159*, <http://pubs.usgs.gov/of/2008/ofr-08-1159>.
- Cascini, L., Cuomo, S., Della Sala, M. (2011). Spatial and temporal occurrence of rainfall-induced shallow landslides of flow type: A case of Sarno-Quindici, Italy, *Geomorphology*, **126** (1-2), 148-158.
- Cascini, L., Cuomo, S., Guida, D. (2008). Typical source areas of May 1998 flow-like mass movements in the Campania region, Southern Italy, *Eng. Geol.*, **96**, 107-125.
- Cuomo, S., Della Sala, M. (2013). Rainfall-induced infiltration, runoff and failure in steep unsaturated shallow soil deposits, *Engineering Geology*, DOI: 10.1016/j.enggeo.2013.05.010.
- Gardner, W. R. (1958). Some steady-state solutions of the unsaturated moisture flow equation with application to evaporation from a water table, *Soil Science*, **85**(4), 228-232.
- Geoslope (2005). User's Guide. GeoStudio 2004, Version 6.13. Geo-Slope Int. Ltd., Calgary, Canada.
- Godt, J.W., Baum, R.L., Savage, W.Z., Salciarini, D., Schulz, W.H., Harp, E.L. (2008). Transient deterministic shallow landslide modelling: requirements for susceptibility and hazard assessments in a GIS framework, *Eng. Geol.*, **102**, 214-226.
- Iverson, R.M. (2000). Landslide triggering by rain infiltration, *Water Resour Res.*, **36**(7):1897–1910.
- Montgomery, D.R., Dietrich, W.E. (1994). A physically-based model for the topographic control on shallow landsliding, *Water Resour Res.*, **30**, 1153–1171.
- Salciarini, D., Tamagnini C. (2014). Physically-based critical rainfall thresholds for unsaturated soil slopes. W. Wu (ed.) Recent advances in modeling landslides and debris flows. *Springer Series in Geomechanics and Geoengineering*, pag. 253 – 264.
- Salciarini, D., Tamagnini, C., Conversini, P., Rapinesi, S. (2012). Spatially distributed rainfall thresholds for the initiation of shallow landslides, *Nat. Haz.*, **61**(1), 229-245.
- Savage, W.Z., Godt, J.W., Baum, R.L. (2003). A model for spatially and temporally distributed shallow landslide initiation by rainfall infiltration, *Proc. of 3rd International conference on debris flow hazards mitigation: mechanics, prediction, and assessment*, Davos, Switzerland, 179–187.
- Sorbino, G., Sica, C., Cascini, L. (2010). Susceptibility analysis of shallow landslides source areas using physically based models, *Nat. Haz.*, **53** (2), 313-332.
- Sorbino, G., Sica, C., Cascini, L., Cuomo, S. (2007). On the forecasting of flowslides triggering areas using physically based models, *Proceedings of the 1st North American Landslides Conference*, AEG Special Publication No. 23. vol. 1, p. 305-315, Editors: V.R. Schaefer, R.L. Schuster, A.K. Turner, ISBN: 9789780975425
- Srivastava, R., Yeh, T.-C.J. (1991). Analytical solutions for one-dimensional, transient infiltration toward the water table in homogeneous and layered soils, *Water Resources Research*, **27** (5), 753–761.